Pullout Resistance of Individual Longitudinal and Transverse Geogrid Ribs

Sidnei H. C. Teixeira[1]; Benedito S. Bueno[2]; and Jorge G. Zornberg, M.ASCE[3]

Abstract: This paper presents an evaluation of the soil-geogrid interaction, conducted to quantify the contributions of passive and interface shear mechanisms to the overall pullout resistance of geogrids. An experimental testing program was conducted in this investigation using both large-scale and newly developed individual-rib pullout devices. The large-scale pullout tests were conducted using uneasily coated geogrid specimens with and without transverse ribs. On the other hand, the individual-rib pullout tests were conducted using individual longitudinal and transverse ribs. A stress transfer model was implemented to predict the results of large-scale pullout tests using the parameters obtained from the individual-rib pullout tests. Good agreement was obtained between the results of large-scale pullout tests and the predictions obtained using parameters collected from individual-rib tests. For the dense mesh geogrids used in this investigation, the development of passive mechanisms in front of geogrid transverse ribs was found to influence significantly the interface shear mechanisms that develop along longitudinal ribs.

DOI: 10.1061/(ASCE)1090-0241(2007)133:1(37)

CE Database subject headings: Pull-out resistance; Geogrids; Soil structure; Reinforcement.

Introduction

The behavior of reinforced soil structures is largely governed by interaction mechanisms that develop between the reinforcement inclusions and the backfill soil. The main function of the inclusions is to redistribute stresses within the soil mass in order to enhance the internal stability of reinforced soil structures. The inclusions undergo tensile strains as they transfer loads from unstable portions of the soil mass into stable soil zones.

The redistribution of stresses within a reinforced soil mass as well as the deformation response of the structure depend on the shear strength properties of the soil, the tensile properties of the inclusions, and the stress transfer mechanism taking place between soil and inclusions. Pullout tests have been typically used to characterize the stress transfer mechanism. While pullout tests provide invaluable information on the overall soil-reinforcement interaction, additional understanding of the multiple mechanisms that occur during pullout testing is still needed and can provide valuable insight into the behavior of reinforced soil structures.

Geogrids are geosynthetic products with comparatively large apertures, which are characterized by a combination of transverse and longitudinal ribs. These ribs provide passive and interface shear contributions, respectively, to the overall geogrid pullout resistance. The experimental program undertaken in this study includes tests conducted using a large-scale pullout device as well as tests conducted using newly developed small-scale devices that allow quantifying the contribution to pullout provided by the geogrid longitudinal and transverse ribs. The results of the testing program allow evaluation of the contribution of the interface shear and passive components to pullout resistance, the effect of spacing between transverse ribs, and the influence of normal stresses on the geogrid response. In order to evaluate the relative contribution of various soil-reinforcement mechanisms, the results obtained from small-scale pullout tests on individual geogrid ribs are also used to predict the pullout test results from large-scale devices using a stress transfer model. The use of small-scale devices, such as those used in this study, allows evaluating the feasibility of obtaining relevant soil-reinforcement interaction parameters using testing procedures that are considerably more expeditious than large-scale pullout tests.

Pullout Mechanisms

The pullout interaction mechanisms between soil and geogrid reinforcements are more complex than those between soil and strip or sheet reinforcements. This is because the pullout resistance of geogrids includes two components: The interface shear resistance that takes place along the longitudinal ribs (and to a lesser extent along the transverse ribs) and the passive resistance that develops against the front of transverse ribs (Koerner et al. 1989). Although the first mechanism could be quantified using parameters obtained from direct shear tests, the latter can only be evaluated using pullout tests. Evaluations of pullout test results have showed that geogrids may develop an equivalent interface shear strength that even exceeds the interface shear strength of the backfill soil (Ingold 1983).

The ultimate pullout resistance has been typically interpreted as the sum of the passive and interface shear components (Jewell

[1]Associate Professor, Dept. of Civil Construction, State Univ. of Londrina, Brazil.

[2]Professor, Dept. of Geotechnical Engineering, Univ. of Sao Paulo, Brazil.

[3]Fluor Centennial Associate Professor, Dept. of Civil, Architectural, and Environmental Engineering, The Univ. of Texas at Austin, Austin, TX 78712.

Note. Discussion open until June 1, 2007. Separate discussions must be submitted for individual papers. To extend the closing date by one month, a written request must be filed with the ASCE Managing Editor. The manuscript for this paper was submitted for review and possible publication on August 26, 2004; approved on March 22, 2006. This paper is part of the ***Journal of Geotechnical and Geoenvironmental Engineering***, Vol. 133, No. 1, January 1, 2007. ©ASCE, ISSN 1090-0241/2007/1-37–50/$25.00.

1996). However, any synergism between these two load transfer mechanisms has often been neglected. Several failure mechanisms have been proposed to estimate the passive pullout resistance that develops against transverse ribs. These include the general shear failure mechanism (Peterson and Anderson 1980), the punching failure mechanism (Jewell et al. 1984), and a modified punching failure mechanism (Chai 1992). The general shear and punching shear failure mechanisms have been reported to provide upper and lower bounds of experimental pullout test results (Palmeira and Milligan 1989a; Jewell 1990b). The interface shear component between geogrid surface and soil has been generally estimated considering the surface area of the geogrid and the interface shear strength properties between the soil and geogrid.

A comprehensive discussion on the prediction of interface shear and passive resistance mechanisms has been summarized by Jewell (1990a) and Bergado et al. (1994). However, many of the available equations correspond to inextensible inclusions and may not rigorously apply to polymeric extensible geogrids. Nonetheless, Milligan and Palmeira (1987) reported good comparison between experimental results and predictions obtained using bearing capacity equations that are valid for rigid reinforcement. Slightly modified analytical procedures were also successfully used to compute the pullout resistance of high-density polyethylene geogrids, as reported by Bergado and Chai (1994) and Alfaro et al. (1995). Teixeira (1999) also showed that experimental results from large-scale pullout tests on polyester geogrids could be predicted within a 10% margin using formulations based on punching failure mechanisms.

Previous studies have reported that the interface and passive resistance contributions to the total pullout resistance depend on the geogrid geometry, soil grain size distribution, and soil density. Specifically, Jewell (1990a) and Bergado et al. (1993) reported that geogrid pullout failure mechanism is a function of the ratio between transverse rib spacing (S) and the transverse rib diameter, the average particle size (D_{50}), the compaction moisture content and the soil stiffness. Jewell (1990a) identified limiting values of the S/D_{50} ratio that characterize either interface shear or full interaction mechanisms (i.e., interface shear plus passive resistance). Additional studies on the variables governing the pullout resistance of geogrids were reported by Sarsby (1985), Lopes and Ladeira (1996), Ochiai et al. (1996), Teixeira and Bueno (1999), and Sugimoto et al. (2001).

An important aspect that can affect the pullout mechanism of geogrids is the interference that transverse ribs may have on the interface shear resistance component (Dyer 1985; Palmeira and Milligan 1989b). For example, the interference between transverse and longitudinal ribs in rigid metal grids buried in dense sand was reported to be function of the geogrid length, spacing between transverse ribs and thickness of transverse ribs (Palmeira 1987; Palmeira and Milligan 1989b). Such interference has been attributed to an increased localized vertical stresses towards the front of the transverse ribs as well as to a decrease in vertical stresses developing behind the transverse ribs (Palmeira 2004). Studies conducted using a variety of geogrid types and mesh densities have focused on quantifying the various pullout mechanisms (Palmeira and Milligan 1989b; Bergado and Chiai 1994; Alfaro et al. 1995; Lopes and Ladeira 1996; Ochiai et al. 1996; Teixeira and Bueno 1999; Sogimoto et al. 2001). However, interpretation of pullout test results continues to be a difficult task, mostly due to can be attributed to complications in quantifying the synergism between interface shear and passive resistance mechanisms.

The study reported in this paper presents an evaluation of the soil-geogrid interaction, conducted to quantify the interface shear and passive contributions to the overall pullout resistance of geogrids. Unlike previous studies, experimental data was obtained not only from conventional pullout tests but also from pullout tests conducted on individual transverse and longitudinal ribs. This allows quantification of the contributions by different pullout mechanisms using a stress transfer model.

Overview of the Testing Equipment

Three different pullout devices were used in the experimental component of this study. This included a large-scale and two individual-rib pullout devices. The results from the large-scale pullout testing program were used to generate experimental results used as reference for subsequent predictions. The results from the individual-rib pullout testing program were used to obtain resistance parameters from isolated longitudinal and transverse ribs of geogrids to be used in a stress transfer model.

Large-Scale Pullout Device

The potential synergism between transverse and longitudinal ribs during pullout testing has led to specific requirements regarding the geometry and dimensions of pullout testing equipment (e.g., Raju et al. 1998). ASTM D6706 (ASTM 2001a) prescribes that the dimensions of large-scale pullout test boxes should exceed 610 mm long, 410 mm wide, and 300 mm high. According to this standard, the box thickness should also exceed 20 times the D_{85} of the soil or 6 times the maximum soil particle size. Finally, the box length should also exceed 5 times the maximum size of the geogrid apertures.

The large-scale pullout device used in this study (Fig. 1) consists of a rigid box, reinforced with U-shaped steel beams (Teixeira and Bueno 1999). Although this study was initiated before ASTM D6706 was adopted, the dimensions of the box used in this study (1,500 mm long, 700 mm wide, and 480 mm high) exceed those prescribed by ASTM D6706. A steel frame was used to support an electric motor that applies the pullout load. The system is capable of applying a tensile force of up to 60 kN to a geosynthetic specimen. A displacement rate of 4.6 mm/min was adopted for the testing program conducted in this study. The normal load was applied using an air bag, which provided a uniform surcharge that was considered representative of field conditions. Two polyethylene membranes, lubricated with grease, were placed against the internal faces of the walls of the equipment in order to minimize side effects during pullout testing.

Data collected during large-scale pullout testing included: (1) pullout force, (2) normal stress applied to the soil surface, (3) localized vertical soil stresses measured using two total stress cells buried within the soil (approximately 10 mm above the geogrid), and (4) longitudinal displacements, measured using six linear variable displacement transformers (LVDTs) connected to various locations along the geogrid specimen using inextensible strings. Fig. 2 shows a view of the large-scale pullout device used in this investigation.

Individual-Rib Pullout Devices

Small-scale pullout devices were developed as part of this investigation to test individual longitudinal and transverse geogrid ribs. These tests were conceived with the objective of providing both

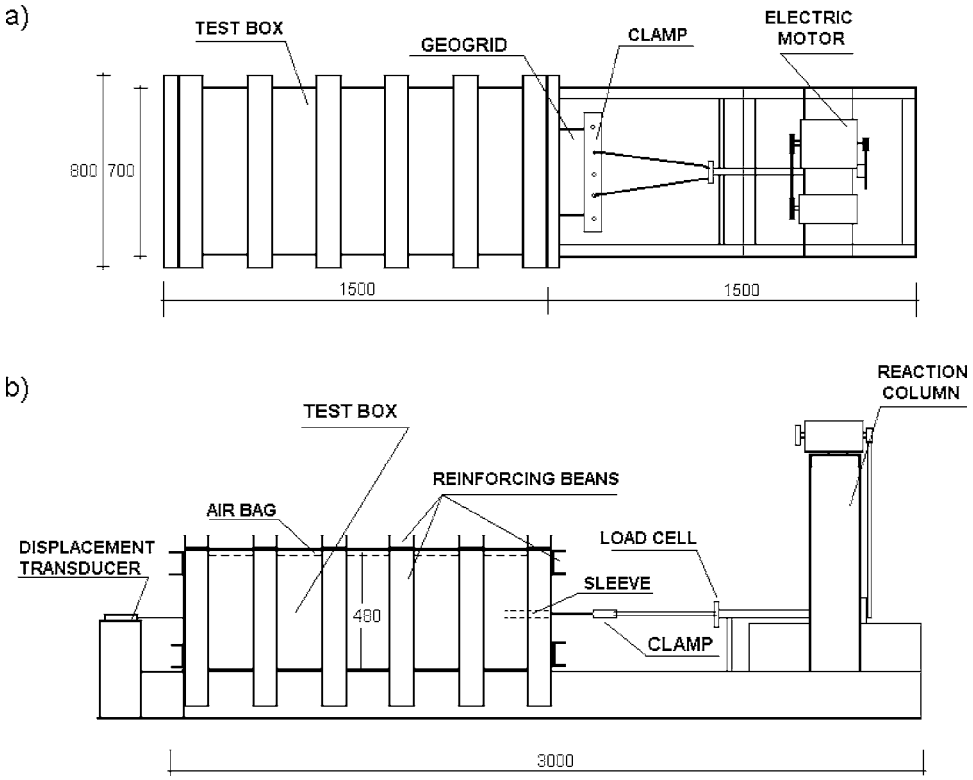

Fig. 1. Schematic view of large-scale pullout test device: (a) plan view; (b) elevation view (note: dimensions are in millimeters)

qualitative and quantitative information on the various mechanisms contributing to the pullout resistance of geogrid reinforcements. Accordingly, the individual-rib pullout tests allowed measurement of the pullout force resulting from applying a constant displacement rate to either longitudinal or transverse geogrid ribs.

Current recommendations for minimum dimensions of pullout devices are not expected to apply to individual-rib pullout devices. This is because the comparatively large dimension requirements for pullout devices (e.g., in ASTM D6706) are needed to capture the interactions among the longitudinal and transverse ribs when testing geogrid reinforcements. Such interactions are not present when testing individual ribs in small-scale pullout devices. A preliminary basis for the minimum dimensions of individual-rib boxes can be drawn from the dimensions of direct shear boxes used to evaluate the interface shear strength between soil and geosynthetics. For example, Mitchell et al. (1990) drew important conclusions on the interface shear strength between soil and various geosynthetics using direct shear tests conducted using 70 mm $\times$ 70 mm geosynthetic samples. The minimum dimensions of the longitudinal-rib pullout tests developed as part of this study are 120 mm in the direction of loading and 70 mm in the transverse direction whereas the minimum dimensions of the transverse-rib pullout tests are 140 mm in the direction of loading and 28 mm (i.e., one rib long) in the transverse direction. As will be discussed in the analysis of the results, additional evidence on the adequacy of the dimensions of the individual-rib devices is provided by the good comparison obtained between the results of small-scale longitudinal-rib pullout tests and large-scale pullout tests conducted on geogrid specimens without transverse ribs.

Fig. 2. View of large-scale pullout test device used in this study

The longitudinal-rib pullout tests were conducted using the pullout box illustrated in Fig. 3, which is 120 mm long, 70 mm wide, and 50 mm high. The tests were conducted using 100-mm-long longitudinal geogrid ribs. The testing procedure involved placing the box at the base of a tensile testing loading frame with the longitudinal geogrid rib aligned vertically and secured with a clamp. As illustrated in Fig. 3(a), a uniform normal stress was applied using an air bag. Use of this pneumatic system for normal load application allowed good control of the normal stress during testing, even when the soil showed dilatancy or contraction during shearing. Lubricated polyethylene films were used along the side walls of the boxes in order to minimize friction between the soil and side walls. The pullout force and the imposed displacements were monitored during testing.

The transverse-rib pullout tests were conducted using the pullout box illustrated in Fig. 4, which is 140 mm long, 28 mm wide, and 50 mm high. The tests were conducted using two transverse ribs placed at the same spacing as in the geogrid where they were obtained from. The transverse-rib pullout tests were also conducted by securing the box on a tensile testing machine and attaching the transverse geogrid ribs to a specially designed

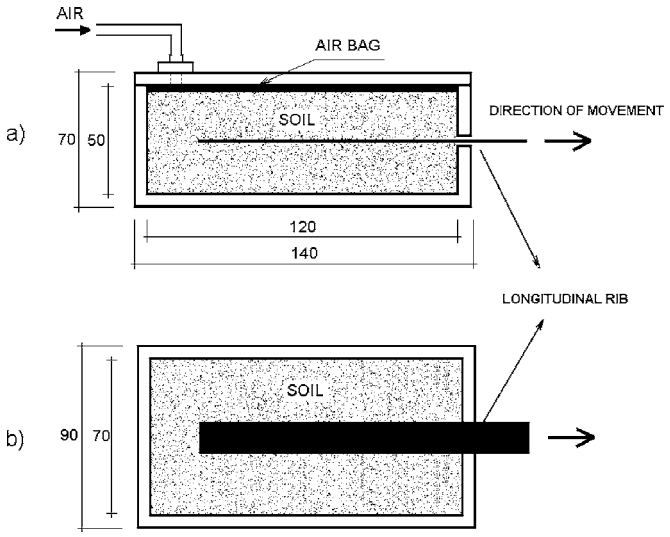

Fig. 3. Schematic views of the longitudinal-rib pullout test device: (a) elevation view; (b) plan view (note: dimensions are in millimeters)

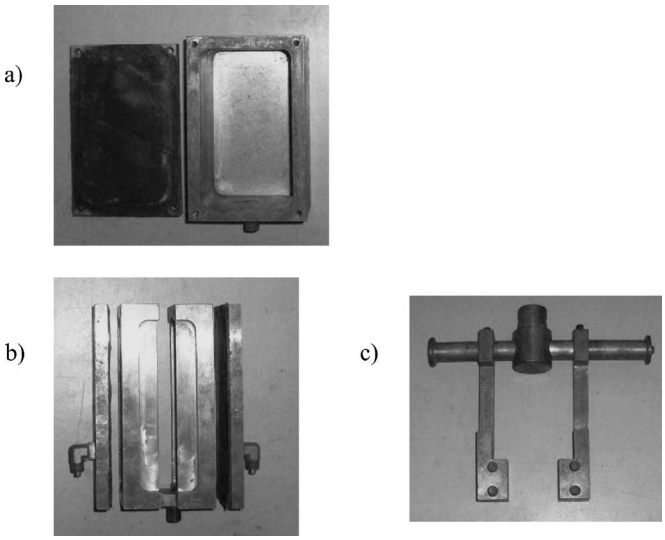

Fig. 5. View of the individual-rib pullout devices: (a) longitudinal-rib pullout box; (b) transverse-rib pullout box; and (c) grip for transverse-rib pullout device

clamping system. As illustrated in Fig. 4(a), a uniform normal stress was applied during testing using two air bags. Also in this case, use of a pneumatic normal loading system allowed good control of normal stress and vertical displacement (dilatancy or contraction) of the soil during transverse-rib pullout testing. Two layers of polyethylene film, lubricated with grease, were installed against the sidewalls. The two clamps developed for this device, each securing one of the ribs, were connected to the same arm. This led to a uniform displacement rate being applied to the extremities of the two transverse ribs [Fig. 4(b)]. The pullout force applied to the second transverse rib [Transverse rib 2 in Fig. 4(b)] was measured during testing using a load cell. The load in the second rib was expected to better account for the interaction between successive transverse ribs in geogrid reinforcements. The original design for the transverse-rib pullout test included only one air bag. However, unlike tests conducted on the longitudinal-rib pullout device, preliminary transverse-rib pullout tests showed some difficulty in controlling the normal load in cases involving significant soil dilatancy. Consequently, the original design of the transverse-rib pullout device was modified by incorporating a second air bag, as shown in Fig. 4(a). This modification proved effective in adequately controlling the applied normal stress. Fig. 5 shows a view of the small scale pullout devices. Specifically, Fig. 5(a) shows a view of the longitudinal-rib pullout device, Fig. 5(b) shows a side view of the transverse-rib pullout device, and Fig. 5(c) shows the grips used in the transverse-rib pullout system.

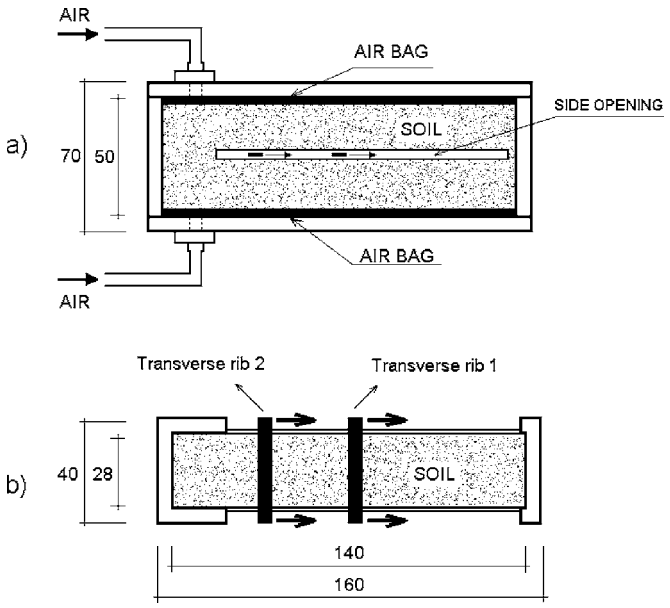

Fig. 4. Schematic views of the transverse-rib pullout test device: (a) elevation view; (b) plan view (note: dimensions are in millimeters)

A load frame with a capacity of 30 kN was used to perform both the longitudinal- and transverse-rib pullout tests (DL 3000, manufactured by EMIC Ltda., São José dos Pinhais-PR, Brazil). The system allowed automatic control of the displacement rate imposed during pullout testing. Conventional clamps were used for the longitudinal-rib pullout tests while customized clamps were used for the transverse-rib pullout tests. Consistent with the displacement rate used for the large-scale pullout tests, a constant displacement rate of 4.6 mm/min was adopted for the longitudinal- and transverse-rib pullout tests.

Pullout load versus displacement curves were generated using the longitudinal- and transverse-rib pullout devices. This provided not only qualitative but also quantitative information on the two mechanisms contributing to the overall pullout resistance of geogrids. In addition, data collected using the individual-rib pullout devices served as input for a stress transfer model used subsequently to predict the pullout resistance obtained from large-scale pullout devices.

Materials

Soils

Two soils were used in the pullout testing program conducted as part of this study. Most tests were conducted using a non-plastic

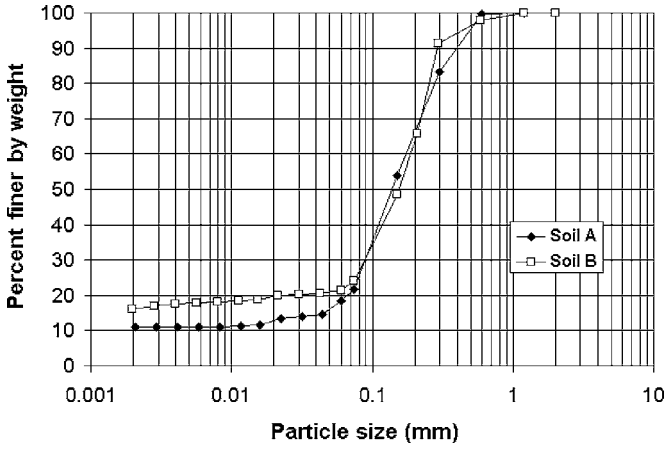

Fig. 6. Particle size distribution of soils used in this study

sandy soil, Soil A, which classifies as SM-SP according to the Unified Soil Classification System. Additional large-scale pullout tests were conducted using Soil B, which classifies as SM according to the USCS. Both soils present a similar grain size distribution, as shown in Fig. 6. The physical characteristics, shear strength parameters, and placement conditions of the soils used in this investigation are listed in Table 1. The shear strength parameters of Soils A and B listed in Table 1 were determined using direct shear tests conducted using soil specimens prepared using the same relative compaction and placement moisture content as the specimens prepared for the pullout testing program.

Geogrids

Two geogrids, identified as G1 and G2, were used in this investigation. Specifically, the geogrid products were uniaxial polyester geogrids coated with PVC. They are manufactured by Huesker Synthetic GmbH and commercialized as Fortrac 200/35-30 and 110/30-20. Geogrid G1 has a rectangular mesh configuration with 29×28 mm internal openings. The longitudinal and transverse ribs of Geogrid G1 are 8 and 3 mm wide, respectively. The fraction of the solid area of Geogrid G1 in relation to its total area, α_s, is 0.29. Some of the large-scale pullout tests were conducted using Geogrid G1 with its transverse ribs removed ($\alpha_s=0.22$). Geogrid G2 has a rectangular mesh configuration with 20×18 mm internal openings. The longitudinal and transverse ribs of Geogrid G2 are 7 and 3 mm wide, respectively, leading to a solid area fraction $\alpha_s=0.37$. The thickness of transverse ribs for both geogrids is 1.5 mm. Fig. 7 presents the unit tension versus strain curves for Geogrids G1 and G2, as obtained from tensile tests conducted in agreement with ASTM D 6637 (ASTM 2001b). The unit tension value reported in Fig. 7 is normalized by the unit width by accounting for the spacing between geogrid longitudinal ribs. As shown in the figure, the geogrids show an approximately linear load-displacement response until rupture.

Table 1. Soil Characteristics

Property	Soil A	Soil B
Specific gravity, G_S	2.664	2.666
Liquid limit, w_L (%)	—	18
Plastic limit, w_P (%)	NP[a]	14
Maximum dry unit weight, $\gamma_{d,\max}$ (kN/m^3)[b]	18.85	19.16
Optimum water content, w_{op} (%)[b]	10.2	10.7
Friction angle, ϕ (°)	36	33
Cohesion, c (kPa)	15	25
Degree of compaction (%)	100	95
USCS soil classification	SM-SP	SM

[a]NP=nonplastic soil.

[b]In relation to Standard Proctor test (ASTM D 698).

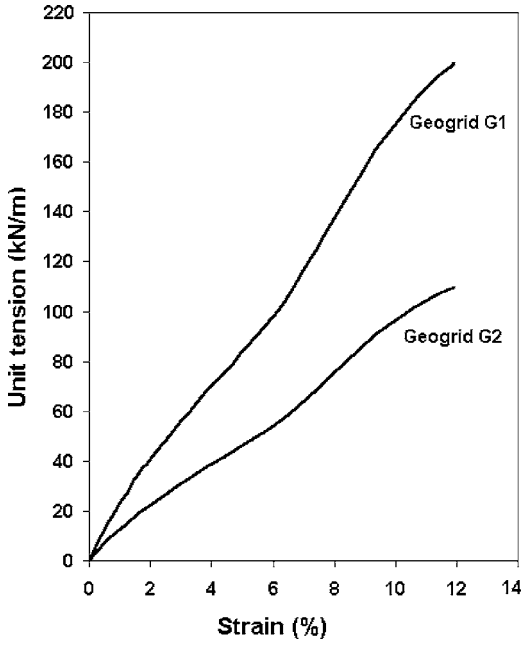

Fig. 7. Results of tensile tests on Geogrids G1 and G2

Testing Procedures

Large-Scale Pullout Tests

The specimens used for the large-scale pullout testing program were prepared by compacting the soil to the target unit weight and moisture content within the pullout box. The weight of moist soil required to achieve the target dry unit weight was initially prepared and homogenized. Compaction was subsequently conducted using a manual hammer with a circular base of 120 mm in diameter and a weight of 60 N, dropped from a height of 300 mm until reaching the target unit weight. The soil was compacted in six 75-mm-thick layers. After placing the initial three layers, the geogrid specimen was positioned within the box and attached to the clamp used to apply the pullout force.

Six inextensible tell-tail strings were used to monitor the internal displacements along the reinforcement. Specifically, displacements of the geogrids were monitored at 33, 264, 495, 726, 957, and 1,188 mm from the front of the specimen using six LVDTs. The strings were encased within polyethylene tubes placed along the reinforcement to minimize friction. In addition, two total stress cells were positioned within the soil mass, 10 mm above the geogrid, to monitor the development of localized normal stresses within the soil mass.

After placement of the geogrid, the upper portion of the box was filled with soil compacted following the same procedures used in the three initial layers. An air bag was installed over the soil surface before placing the top cover. Use of a pneumatic system for normal loading facilitated applying a uniformly dis-

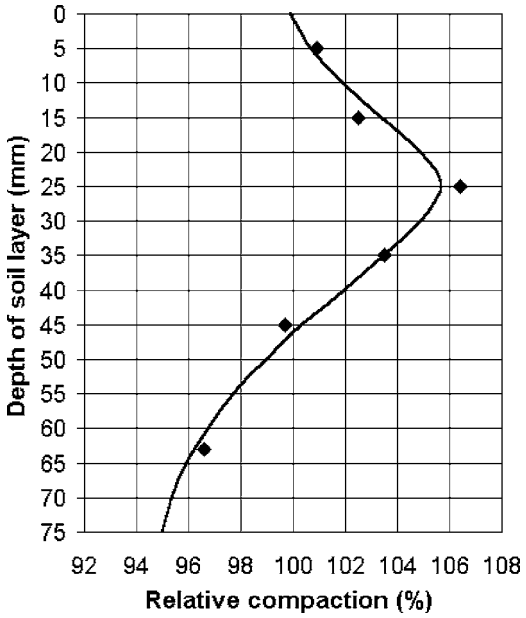

Fig. 8. Profile of relative compaction within a 75 mm thick layer (Soil A)

tributed pressure, which was applied using a compressor controlled by a regulator. The applied load and the displacements in the six tell-tails were monitored until the ultimate pullout resistance was achieved.

Individual-Rib Pullout Tests

The specimens for the individual-rib pullout tests were prepared by compacting the soil to the target unit weight and moisture content within the small-scale boxes using 12.5-mm-thick layers. Soil compaction was conducted by tamping using a 10 N manual hammer with a square base of 20-mm-long sides. The hammer was dropped from a height of 100 mm until reaching the target unit weight. The compaction procedures used in individual-rib tests were consistent with those used in the large-scale pullout tests and aimed at obtaining comparable soil conditions in the various pullout devices. As the compaction profile is a function of the layer thickness, a special compaction control procedure was implemented to replicate the density profile achieved in large-scale pullout tests into the vicinity of the upper and lower soil-geogrid interfaces. Specifically, the soil density profile in the large-scale pullout box prepared using 75-mm-thick compacted soil layers was evaluated with the objective of reproducing the same conditions in the individual-rib pullout tests. Fig. 8 shows the density profile (shown as relative compaction in relation to Standard Proctor maximum dry unit weight) in a 75-mm-thick layer compacted to achieve a target density corresponding to 100% relative compaction. As shown in the figure, the relative compaction is approximately 100% towards the top of the layer, it reaches approximately 106% in the upper third portion of the compacted layer, and it decreases to a relative compaction of approximately 95% toward the base of the compacted layer. While the relative compaction profile shown in Fig. 8 is a function of the soil type, compaction equipment and compaction procedures, similar profiles were expected for the specimens prepared for the large-scale pullout testing program conducted as part of this investigation. In order to reproduce the compaction conditions obtained in the large-scale pullout specimens into the individual-rib pullout specimens, the bottom layers of the small-scale specimens were compacted to a target relative compaction of 100%, whereas the upper layers were compacted to a target relative compaction of 95%.

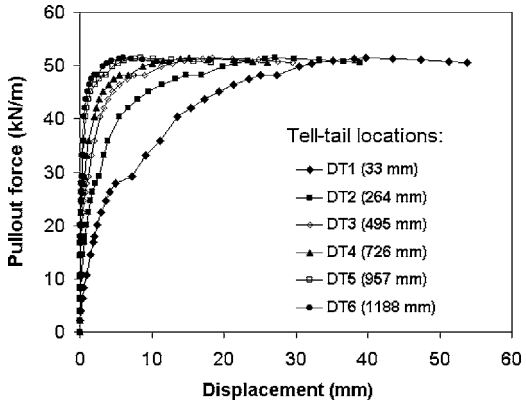

Fig. 9. Load-displacement curves from tell-tails located along the geogrid specimen in a large-scale pullout test (Test LS3)

The internal walls of the individual-rib pullout boxes were lined using lubricated polyethylene membranes in order to minimize side friction during testing. After preparing of the two bottom soil layers, the individual ribs were placed in the boxes following the layout shown in Figs. 3 and 4 for the longitudinal- and transverse-rib pullout tests, respectively. The two top soil layers were subsequently placed over the individual rib elements. The air bag and top cover plate of the small-scale boxes were subsequently installed. The individual-rib pullout boxes were placed in the load frame and the geogrid ribs were subsequently fixed to the clamping system. Individual-rib pullout tests were conducted using a constant displacement rate of 4.6 mm/min. An automated data acquisition system was used to collect displacement and pullout force during testing. The repeatability of the new testing procedures was evaluated by performing a series of conformance tests, which lead to coefficients of variation of 4 and 6% for longitudinal- and transverse-rib pullout tests, respectively. All instruments, load cells, pressure cells and displacement transducers, were periodically calibrated following manufacturer's procedures. The individual-rib pullout tests were expeditious, particularly when compared with large-scale pullout tests. While sample preparation and testing of large-scale pullout tests would typically take 3–4 days, individual-rib pullout tests would be typically accomplished in less than 4 hours.

Test Results and Analysis

Scope of the Testing Program

A combination of large-scale and individual-rib pullout tests was performed with the objective of estimating the contribution of the different mechanisms to the pullout resistance of geogrids. The several types of pullout tests were conducted using normal stresses of 25 and 50 kPa. The large-scale pullout tests were conducted using Geogrids G1 and G2, whereas the individual-rib pullout tests were conducted using Geogrid G1. Large-scale pullout tests were also conducted using geogrids with their transverse ribs removed in order to evaluate the contribution of the interface shear resistance mechanism to the overall pullout resistance. By comparison with results obtained from longitudinal-rib pullout

Table 2. Scope of Large-Scale Pullout Testing Program

Test	Geogrid	Soil	Normal stress (kPa)	Length (mm)	Spacing between transverse ribs (mm)
LS1	G1	A	25	350	32
LS2	G1	A	25	600	32
LS3	G1	A	25	1,200	32
LS4	G1	A	50	600	32
LS5	G1	A	25	600	No transverse ribs
LS6	G2	B	25	600	22
LS7	G2	B	25	600	44
LS8	G2	B	25	600	66

tests, the results from large-scale pullout tests with specimens without transverse ribs also allowed evaluation of the potential effect of box size on the small-scale pullout test results. In addition, large-scale pullout tests were also conducted using geogrids with a fraction of the transverse ribs removed in order to evaluate the effect of transverse rib spacing. The spacing between ribs in the transverse-rib pullout tests was 28 mm, which corresponds to the transverse rib spacing of the original geogrid. Tables 2 and 3 summarize the scope of the large-scale and individual-rib pullout testing programs.

Large-Scale Pullout Test Results

Fig. 9 shows the results obtained from a typical large-scale pullout test (Test LS3, see Table 2). Fig. 9 shows the applied pullout force as a function of internal displacements, measured using tell tails attached at different locations within the geogrid specimen. Fig. 10 shows the displacement profiles along the geogrid length for Pullout Test LS3. The profiles are presented for increasing values of the pullout force, which is shown in Fig. 10 as a percentage of the maximum pullout resistance. The maximum displacement occurs at the point of application of the pullout load and decreases towards the back of the geogrid following a nonlinear trend that reflects the effect of reinforcement extensibility.

Fig. 11 presents the localized normal stresses, as measured by two total stress cells (TSC1 and TSC2) located approximately 10 mm over the soil-geogrid interface (Test LS3). The total stress cells have a diameter of 28 mm and were aligned at the central portion of the geogrid apertures (in between two longitudinal ribs). Cell TSC1 was initially located in between two transverse ribs (at a distance of 528 mm from the point of application of the pullout load), whereas Cell TSC2 was initially located directly

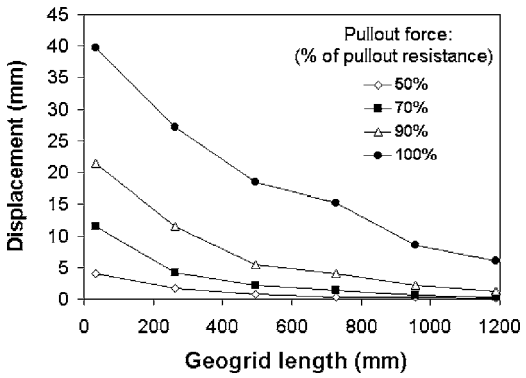

Fig. 10. Distribution of displacements along the geogrid (Test LS3)

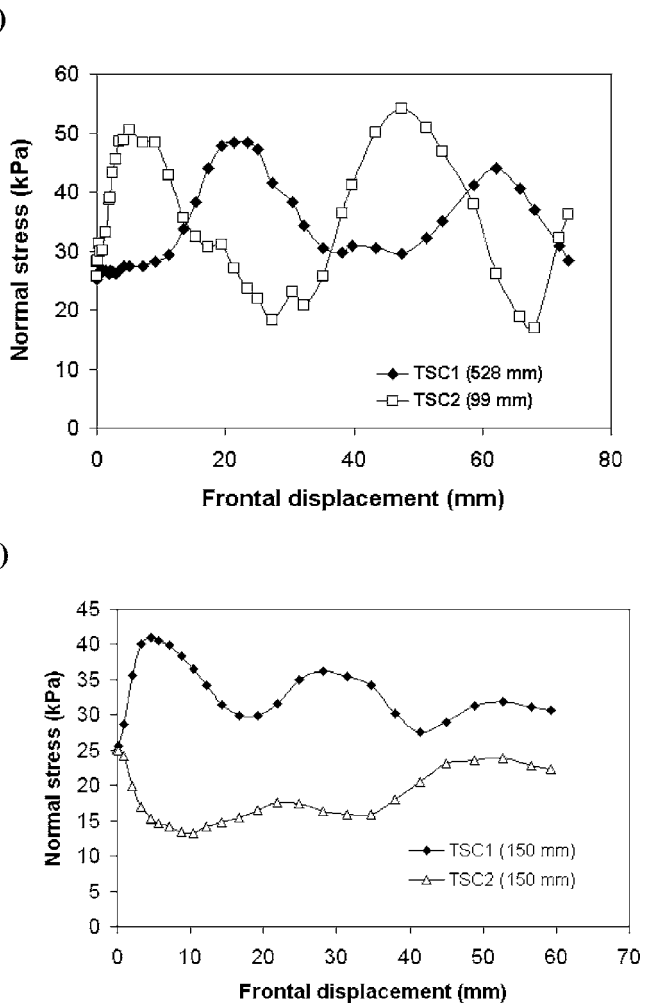

Fig. 11. Localized normal stresses in the vicinity of soil-geogrid interface: (a) measured using stress cells located between longitudinal ribs; (b) measured using stress cells located between and directly over longitudinal ribs

over a transverse rib (at a distance of 99 mm from the point of load application). The cell active area covers practically the entire geogrid opening area (28×29 mm). The localized normal stresses in the beginning of the test (i.e., for zero frontal displacement) correspond to the applied normal stress of 25 kPa. However, as the test progresses, the localized stresses measured by the total stress cells oscillate and show normal stress values ranging from approximately 10 to 50 kPa. It should be noted that the distance between peaks in the measured localized stresses is consistent with the spacing between transverse ribs of the Geogrid G1 used in Test LS3 (i.e., 32 mm, as shown in Table 2).

The soil in front of the transverse ribs is displaced over and under the transverse ribs during pullout testing, which causes a tendency toward dilation over the transverse ribs (Dyer 1985). As dilation is partially inhibited, the normal stresses tend to increase in the vicinity of the transverse ribs and tend to decrease in between transverse ribs. This is consistent with the oscillation of normal stress measurements shown in Fig. 11(a), where the soil directly over transverse ribs is overstressed, whereas the soil in the zone between transverse ribs (i.e., over the apertures) shows a comparative decrease in normal stress. It should be noted that the measurements shown in Fig. 11(a) correspond to stress cells aligned with the geogrid apertures (between two longitudinal

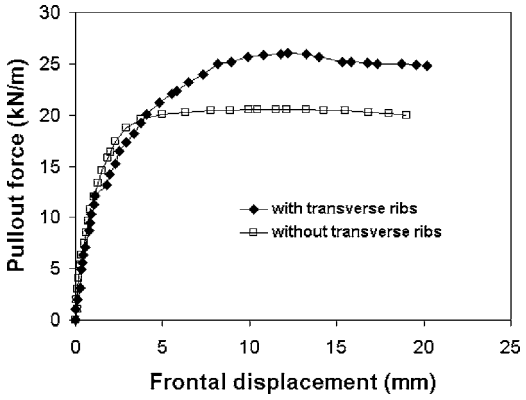

Fig. 12. Results of pullout tests conducted using geogrids with and without transverse ribs

ribs). Accordingly, the localized normal stresses oscillate around an average normal stress value that exceeds the applied normal stress of 25 kPa. To compensate for the relative increase in normal stress observed along the geogrid apertures (between two longitudinal ribs), a relative decrease in normal stress in relation to the applied normal stress should take place along the geogrid longitudinal ribs. This can be observed in Fig. 11(b), which shows the oscillation of localized normal stresses around an average normal stress value that is below the applied normal stress of 25 kPa. In this case, the total stress cells were placed at the same distance from the point of load application (150 mm) but Cell TSC1 was located between two longitudinal ribs, whereas Cell TSC2 was located directly over a longitudinal rib. As shown in Fig. 11(b), the relative decrease in localized normal stresses along the longitudinal ribs was confirmed by the measurements of Load Cell TSC2. This suggests that the presence of transverse ribs not only induces the development of zones with localized normal stress variations, but that the localized redistribution of normal stresses appears to have a detrimental effect on the interface shear resistance component that develops along longitudinal ribs.

The progressive nature of passive resistance mobilization along the geogrid length and interference between ribs is consistent with the photoelastic observations of the pullout response of geogrids reported by Milligan et al. (1990). This study reported that passive resistance mobilization reduced the interface shear mobilization between soil and transverse ribs and, to a certain extent, between soil and longitudinal ribs. This is also consistent with observations reported by Palmeira (2004), who indicated that the fraction of the ultimate pullout resistance due to interface shear may be significantly smaller than that due to passive mechanisms.

Fig. 12 compares the results of Pullout Tests LS2 and LS5, conducted using Geogrid G1 with and without transverse ribs. The tests were conducted using a normal stress of 25 kPa. As shown in Fig. 12, the pullout resistance of the geogrid with transverse ribs is higher than that of the geogrid without transverse ribs. As the pullout resistance of the geogrid with transverse ribs is only 26% higher than that of the geogrid without transverse ribs, a cursory interpretation of these results could erroneously suggest that the passive resistance mechanisms provides only a comparatively small contribution to the overall pullout resistance. However, the pullout resistance of geogrids without transverse ribs should not be considered representative of the contribution of interface shear to the pullout resistance of geogrids. This is because, as will be discussed in the evaluation of individual-rib

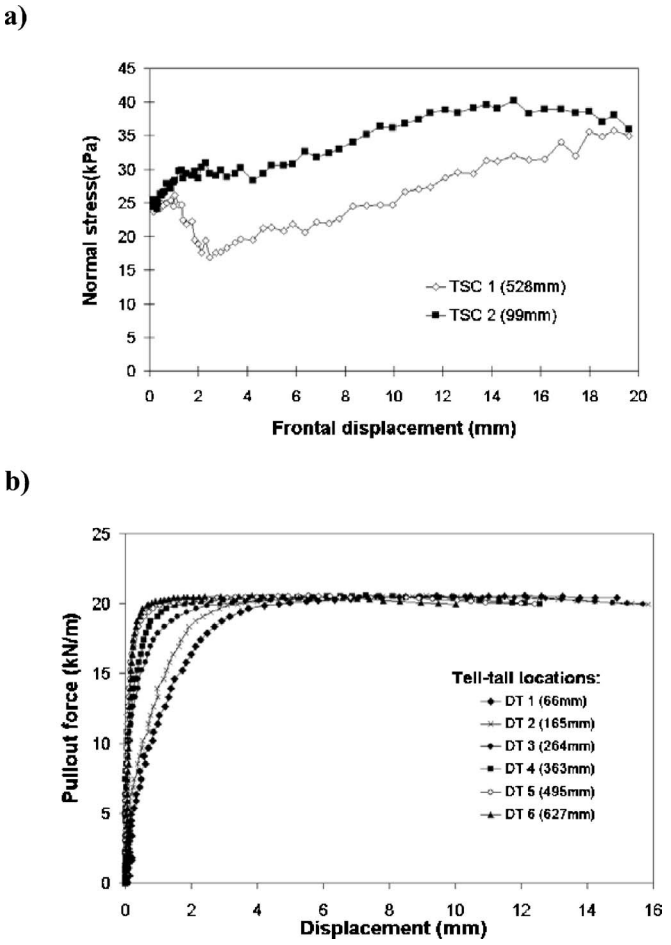

Fig. 13. Experimental results from pullout test conducted using a geogrid specimen without transverse ribs (Test LS5): (a) localized normal stresses in the vicinity of soil-geogrid interface; (b) load-displacement curves from tell-tails located along the geogrid specimen

pullout tests, the contribution of interface shear to the geogrid pullout resistance may be significantly reduced due to the interaction between longitudinal and transverse ribs.

Additional insight on the pullout behavior of geogrids can be obtained by evaluating measurements of localized normal stresses, as obtained from total stress cells placed on tests with and without transverse ribs. Fig. 13(a) shows the localized normal stresses measured in Test LS5 performed using a geogrid speci-

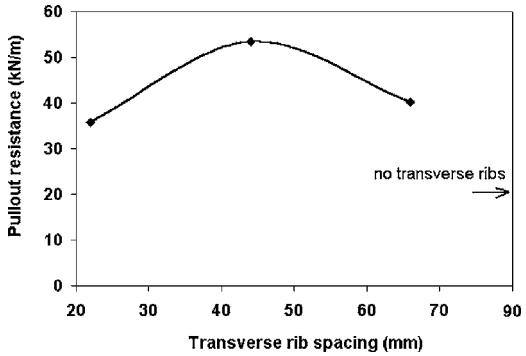

Fig. 14. Effect of transverse-rib spacing on pullout resistance

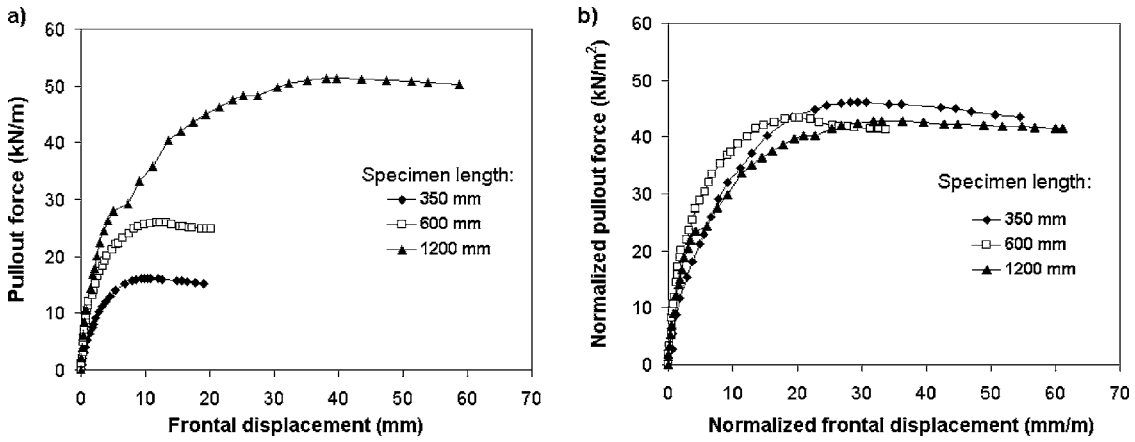

Fig. 15. Effect of specimen length on pullout resistance: (a) force versus displacement curve; (b) normalized force versus displacement curve

men without transverse ribs. The measurements were obtained using total stress cells placed directly over a longitudinal rib at 528 and 99 mm from the point of application of the pullout force. As shown in Fig. 13(a), oscillations of localized normal stress do not take place as the test progresses. However, the localized normal stresses are also observed to increase with increasing pullout displacement, reaching a magnitude of approximately 38 kPa (i.e., a value 52% higher than the applied normal stress). Fig. 13(b) shows the applied pullout force as a function of the internal displacements measured using tell tails attached at different locations within the geogrid specimen. The increased localized normal stress that develops with increasing displacements can be attributed to the effect of inhibited dilatancy of the soil in vicinity of longitudinal ribs. Unlike the normal stress oscillations observed in the test conducted using a geogrid with transverse ribs, the localized normal stresses reach constant value at large displacements in the test conducted using a geogrid without transverse ribs. Consequently, no detrimental effect due to normal stress relief along the longitudinal ribs is observed in the absence of transverse ribs.

Additional large-scale pullout tests were performed to study the effect of spacing between geogrid transverse ribs, S (Tests LS6, LS7 and LS8 in Table 2). The geogrid specimens were prepared by removing the transverse ribs from Geogrid G2, which has an original transverse rib spacing of 22 mm. Pullout tests were then conducted using Geogrid G2 with transverse rib spacings of 22, 44, and 66 mm. Fig. 14 shows the results from tests performed with the different geogrid mesh densities. Although a decreasing pullout resistance is expected for increasing transverse rib spacing, the results in Fig. 14 show that there is an optimum spacing that maximizes the pullout resistance. When the transverse rib spacing is below the optimum value, the pullout response appears to be detrimentally affected by the effect that transverse ribs cause on the interface shear component of the pullout resistance. On the other hand, when the transverse rib spacing is above the optimum value, the pullout resistance is comparatively decreased because of the small number of transverse ribs that provide passive resistance contribution to the overall pullout resistance. These results highlight the significant effect of transverse rib spacing on the overall pullout resistance of polymeric geogrids.

Large-scale pullout tests were also performed with the objective of evaluating the effect of the geogrid length on the pullout resistance. Specifically, Tests LS1, LS2, and LS3 (see Table 2) were performed using Geogrid G1 with specimen lengths of 350, 600, and 1200 mm. The tests were conducted using Soil A and a normal stress of 25 kPa. Fig. 15(a) shows the results of this pullout testing program. As shown in Fig. 15(a), an increasing specimen length leads to increasing pullout resistance, increased initial stiffness, and increased displacement at peak pullout resistance. It should be noted that the pullout resistance increases approximately linearly with the geogrid specimen length. Indeed, the three pullout force-displacement curves appear to collapse into a single normalized curve when the pullout force and the frontal displacement are normalized in relation to the specimen length [Fig. 15(b)]. This normalized response should not be assumed for conditions other than those used in this study without careful consideration of the extensibility of the geogrids. However, at

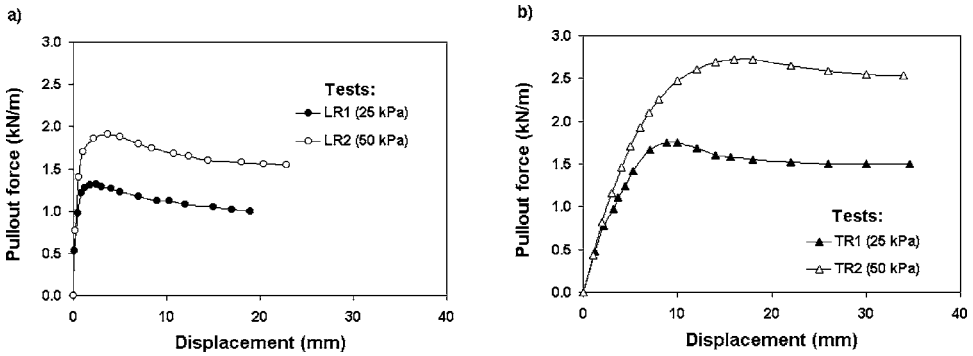

Fig. 16. Results of individual pullout tests: (a) longitudinal-rib pullout tests; (b) transverse-rib pullout tests

Table 3. Scope of Individual-Rib Pullout Testing Program

Test	Type of pullout test	Geogrid	Soil	Normal stress (kPa)
LR1	Longitudinal rib	G1	A	25
LR2	Longitudinal rib	G1	A	50
TR1	Transverse rib	G1	A	25
TR2	Transverse rib	G1	A	50

least for the conditions considered in this pullout testing program, the pullout resistance was found to be directly proportional to reinforcement length in spite of the complex stress transfer mechanisms that take place during pullout testing of geogrids.

Individual-Rib Pullout Test Results

Longitudinal- and transverse-rib pullout tests were conducted using Soil A and individual ribs obtained from Geogrid G1. The specimens were prepared following the previously described procedures. The same materials and soil placement conditions were used in these tests as in the large-scale pullout tests to allow comparison of the test results. Fig. 16(a) presents the results of the longitudinal-rib pullout tests summarized in Table 3. The embedment length of the specimens used in the longitudinal pullout tests was 100 mm. However, in order to facilitate comparison with the results from transverse pullout tests, the pullout force values presented in Fig. 16(a) were scaled to represent an embedment length of 32 mm (i.e., the transverse-rib spacing) and a pullout force per unit width (1 m). The tests were performed under normal stresses of 25 and 50 kPa. The longitudinal-rib pullout test results show an initially linear portion, followed by a well-defined peak and a postpeak loss in pullout resistance. The displacement at peak pullout force increases with increasing normal stress.

Fig. 16(b) presents the results of the transverse-rib pullout tests summarized in Table 3. Since the width of the transverse-rib pullout box is 28 mm, the results presented in Fig. 16(b) were scaled to represent the pullout force per unit width (1 m) of geogrid reinforcement. As previously mentioned, the distance between transverse ribs in Geogrid G1 is 32 mm. Consequently, this spacing was used between the two transverse ribs in the individual-rib pullout device. The pullout resistance values reported in Fig. 16(b) correspond to the pullout resistance from Transverse Rib 2 only [see Fig. 4(b)]. The tests were performed under normal stresses of 25 and 50 kPa. As in the longitudinal-rib pullout results, the transverse-rib pullout results present an initially linear portion, followed by a well-defined peak and a postpeak loss in pullout resistance. As transverse ribs reach a displacement of 32 mm, which corresponds to the transverse rib spacing [i.e., as Transverse Rib 2 reaches the initial position of Transverse Rib 1, see Fig. 4(b)], the pullout force reaches an approximately constant value. As in the case of longitudinal-rib pullout tests, the displacement at peak pullout resistance increases with increasing normal stress. However, the magnitude of the displacement at peak obtained in transverse-rib pullout tests is over four times the displacement at peak obtained in longitudinal-rib pullout tests.

A preliminary evaluation of the relative contribution of the longitudinal and transverse ribs to the overall pullout resistance could be made by inspection of the results presented in Figs. 16(a and b). This is because the pullout results shown in Figs. 16(a and b) account for the actual longitudinal- and transverse-rib spacing and have been scaled to the same unit width. However, it should be emphasized that such direct comparison ignores any interference between longitudinal and transverse ribs. As will be discussed, the overall pullout resistance of Geogrid G1 cannot be obtained by directly adding the individual contributions of longitudinal and transverse ribs, measured in individual-rib pullout tests. As previously shown in Fig. 12, the pullout resistance of the geogrid with transverse ribs is only 26% higher than that of geogrids without transverse ribs when tested under a normal stress of 25 kPa. However, it would be erroneous to infer from these results that the relative contribution of transverse ribs to the overall pullout resistance is only 26%. In fact, as shown in Figs. 16(a and b), the results from individual-rib pullout tests conducted using a normal stress of 25 kPa appear to suggest that the contribution of transverse ribs is approximately 60% of the combined interface shear and passive resistance. In summary, the contribution to pullout resistance of individual longitudinal and transverse ribs cannot explain adequately the comparatively small difference in pullout resistance obtained from tests conducted using geogrids with and without transverse ribs. This discrepancy can be qualitatively explained by the localized stress measurements presented in Fig. 11, which suggest that the presence of transverse ribs induces a normal stress relief that affects detrimentally the interface shear resistance contribution of longitudinal ribs.

Prediction of Large-Scale Pullout Behavior Using Individual-Rib Pullout Tests

Stress Transfer Model

An analytical model was implemented as part of this study to predict the experimental results of large-scale pullout tests using results obtained from individual-rib pullout tests and from unconfined geogrid tensile tests. The stress transfer model is consistent with that reported by Bergado and Chai (1994). Other analytical and numerical stress transfer models, which quantify the contributions of the interface shear and passive resistance mechanisms, have also been developed to predict the reinforcement pullout (e.g., Sugimoto et al. 2001; Palmeira 2004; Wilson-Fahmy and Koerner 1993). The general approach involves discretizing the length of the geogrid into segments that are representative of the transverse rib spacing with the overall objective of predicting the pullout force vs. displacement response.

The stress transfer model implemented in this study allows prediction of the displacement, strain and load profiles along the geogrid length. The model also allows prediction of the load versus displacement curve at any point in the geogrid reinforcement, such as at the point of load application. The model was tailored for direct use of the experimental data generated using the longitudinal- and transverse-rib pullout devices developed in this investigation. Specifically, the model requires:

1. The pullout force versus displacement curve obtained from a longitudinal-rib pullout test [Fig. 16(a)];
2. The pullout force versus displacement curve obtained from a transverse-rib pullout test [Fig. 16(b)]; and
3. The unit tension versus strain curve obtained from an unconfined tensile test on a longitudinal rib (Fig. 7).

The stress transfer model represents the geogrid as a sequence of segments, each composted by a longitudinal and a transverse rib (Fig. 17). An iterative solution process allows determination of the force distribution along the geogrid reinforcement that corresponds to a given frontal displacement, Δf. Each segment j of the

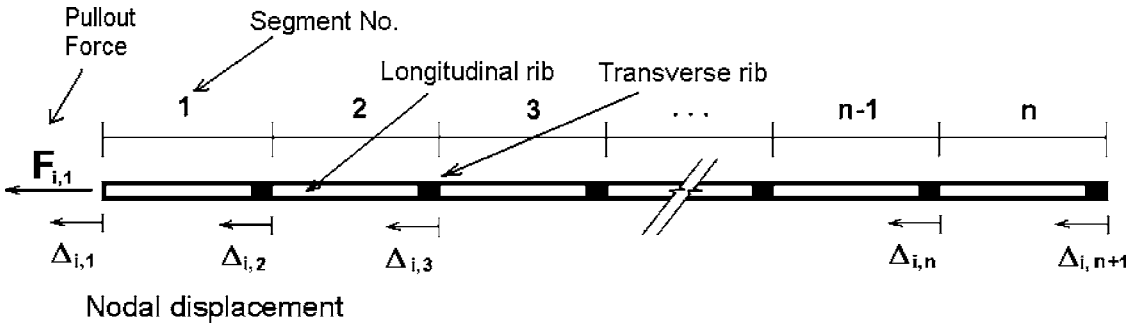

Fig. 17. Definitions used in geogrid stress-transfer model (iteration i)

geogrid is associated to a front displacement, $\Delta_{i,j}$, and back displacement $\Delta_{i,j+1}$, where i=iteration number. The back displacement of each segment should equal the front displacement of the subsequent segment.

For a given frontal displacement, Δf, the frontal force $F_{i,1}$ for iteration i is initially assumed, and the solution process leads to a decreasing nodal force towards the end of the geogrid. The residual force, $F_{i,n+1}$, is eventually calculated for the back node of the last segment, where n=the total number of segments. If the residual force is higher than zero (within a predefined tolerance), a lower value of frontal force $F_{i+1,1}$ should be assumed for the next iteration. Conversely, if the residual force is smaller than zero, a higher value of frontal force should be assumed. The iterative process ends once the residual force in last segment becomes negligible. The specific steps involved in the iterative procedure are as follows:

1. Adopt a frontal displacement, Δ_f.
2. Assume a pullout load $F_{i,1}$ for interaction i, which corresponds to the imposed frontal displacement (i.e., to the frontal displacement $\Delta_{i,1}=\Delta_f$). A preliminary estimate for the initial assumption can be obtained by considering rigid longitudinal ribs, which implies assuming that $F_{1,1}$ equals the summation of loads from all longitudinal and transverse ribs determined from the pullout load vs. displacement curves for a uniform displacement Δ_f acting over the entire geogrid.
3. Obtain the longitudinal-rib pullout resistance, $Rl_{i,1}$, of the first longitudinal rib, by defining the pullout force that corresponds to a displacement $\Delta_{i,1}$ in the longitudinal-rib pullout curve.
4. Compute the average tensile load $T_{i,1}$ acting along Segment 1, as follows:

$$T_{i,1} = F_{i,1} - \beta\, Rl_{i,1}/2 \tag{1}$$

where β=empirical influence factor that ranges from 0 to 1 and accounts for the influence that transverse ribs may have on the interface shear mechanism developed by longitudinal ribs. The value of β depends on the geogrid mesh geometry ($\beta=1$ for open geogrid meshes and $\beta=0$ for dense meshes). While the experimental results obtained in this study involve only comparatively dense geogrid meshes, a generic empirical factor was included in the procedure for completeness. It should be noted that Eq. (1) assumes that $Rl_{i,1}$ varies linearly along the geogrid segment.

5. Obtain the average strain, $\varepsilon_{i,1}$, of the first longitudinal element as the strain corresponds to the average load $T_{i,1}$ in the tensile load vs. strain curve from the unconfined tensile test.
6. Compute the displacement at the back of Segment 1, $\Delta_{i,2}$, as follows:

$$\Delta_{i,2} = \Delta_{i,1} - \varepsilon_{i,1}\, L_{\text{rib}} \tag{2}$$

where L_{rib}=length of the longitudinal rib segment (i.e., the spacing between transverse ribs).

7. Obtain the passive resistance, $Rt_{i,1}$, of the first transverse rib by defining the pullout force that corresponds to displacement $\Delta_{i,2}$ in the transverse-rib pullout curve.
8. Calculate the force, $F_{i,2}$, acting in front of Segment 2 as follows:

$$F_{i,2} = F_{i,1} - \beta\, Rl_{i,1} - Rt_{i,1} \tag{3}$$

9. Using the calculated force and displacement at Node 2 (front of Segment 2), $\Delta_{i,2}$ and $F_{i,2}$, repeat Steps (3)–(8) to obtain the force and displacement at Node 3. Repeat this process $n+1$ times until calculating the pair of values $\Delta_{i,n+1}$ and $F_{i,n+1}$ that correspond to the end values at the geogrid corresponding to interaction i. The average tensile load $T_{i,j}$ acting along Segment j, should be calculated as follows:

$$T_{i,j} = F_{i,j} - \beta\, Rl_{i,j}/2 \tag{4}$$

10. The force at the last node, $F_{i,n+1}$, should be negligible if the initially assumed force at the front node, $F_{i,1}$, is correct. Otherwise, a new iteration should be initiated by assuming a new value of pullout force at the front node, $F_{i+1,1}$. The process should be repeated m times, where m is the iteration number for which the assumed pullout force at the front node leads to a negligible residual force at the last node. The following expression for the assumed pullout force at the front node was found useful to expedite convergence of the iterative process:

$$F_{i+1,1} = F_{i,1} - \frac{F_{i,n+1}}{k} \tag{5}$$

where k=constant ranging from 5 to 20. High values of k facilitate convergence of the iterative process but result in a larger number of iterations.

The above-described procedure should be repeated for several values of imposed frontal displacements Δ_f. The set of imposed displacements, Δ_f, and calculated pullout force at the front node obtained after convergence of the iterative process, $F_{m,1}$, define the predicted pullout load versus frontal displacement curve. In addition, the results obtained after convergence for each imposed frontal displacement can also be used to define load and displacement profiles along the geogrid length at the various stages during pullout testing.

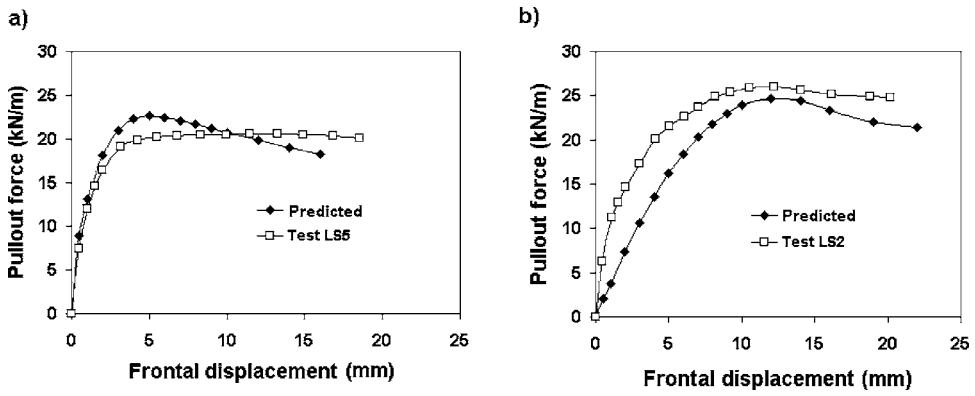

Fig. 18. Comparison between large-scale pullout test experimental results and predictions: (a) Test LS5 and predicted curve; (b) Test LS2 and predicted curve

Comparison between Experimental and Predicted Large-Scale Pullout Results

The stress transfer model allowed prediction of the results obtained from large-scale pullout tests using input from the individual-rib pullout tests [Figs. 16(a and b)] and from the tensile test on longitudinal ribs of Geogrid G1 (Fig. 7). Fig. 18(a) shows the pullout force versus frontal displacement experimental results from the test conducted using a geogrid specimen without transverse ribs (LS5) and the prediction obtained using the results from individual-rib pullout Test LR2. As the transverse ribs of the geogrid specimen used in Test LS5 were removed, the prediction neglected the transverse-rib resistance components (i.e., $Rt_{i,j}=0.0$) and considered an influence factor $\beta=1.0$. As shown in Fig. 18(a), a very good agreement was obtained between the experimental large-scale pullout test results and the predicted values, particularly for displacements up to approximately 3 mm. The good comparison suggests that the small-scale longitudinal-rib pullout tests can be used to predict accurately the large-scale pullout behavior of geogrid reinforcements for cases in which the pullout response is dominated by interface shear mechanisms.

In addition, the good comparison between experimental large-scale pullout test results and predictions using small-scale longitudinal-rib pullout test data also provides evidence of the suitability of the design adopted in this study for the small-scale pullout devices. This is particularly relevant considering that the individual-rib pullout devices are significantly smaller than standard pullout equipment for full (i.e., multiple-rib) geogrid specimens. Consequently, because of the lack of interference in individual-rib pullout tests, these small-scale tests provide an alternative approach for characterization of pullout parameters avoiding the need of comparatively large-scale pullout devices.

As previously discussed, the presence of transverse ribs appears to affect detrimentally the contribution of longitudinal ribs to the overall pullout resistance, at least for the comparatively dense Geogrid G1 used in this study. Indeed, it is expected that the interface shear mechanism would contribute to the overall pullout resistance only for comparatively small displacements while the passive resistance mechanism would contribute to the overall pullout resistance for comparatively large displacements. The passive resistance mechanism would ultimately govern the ultimate pullout resistance for the large displacements that correspond to the peak pullout resistance. Fig. 18(b) compares the experimental results from the large-scale pullout Test LS2 with a prediction obtained using individual-rib tests performed at 25 kPa. This pullout prediction was conducted with the objective of obtaining the peak pullout resistance, which occurs at comparatively large displacements. Accordingly, the prediction shown in Fig. 18(b) was obtained using the stress transfer model and neglecting the interface shear resistance provided by the longitudinal ribs (i.e., considering $\beta=0$). The comparison is reasonably good, particularly for the value of the ultimate pullout resistance. The agreement between the ultimate pullout resistance obtained from large-scale experimental pullout testing and the prediction obtained using small-scale transverse-rib pullout tests confirms that, at least for the comparatively dense Geogrid G1 used in this study, the ultimate pullout resistance is governed by the passive resistance contribution provided by the transverse ribs.

Fig. 19 shows a comparison between the experimental results form the large-scale pullout Test LS2 and a prediction obtained using individual-rib pullout tests performed at 25 kPa. In this case, the objective was to simulate the entire load-displacement curve rather than only to obtain the peak pullout resistance. Accordingly, the influence factor β was backcalculated accounting for the magnitude of displacements at peak observed in the individual-rib pullout tests. The good agreement observed in Fig. 19 was obtained by selecting influence factor β varying linearly from $\beta=0.6$ for a frontal displacement of zero to $\beta=0.0$ for a frontal displacement of approximately 10 mm. A displacement of 10 mm corresponds to the frontal displacement at peak pullout obtained from transverse-rib pullout tests. The good comparison obtained for the entire pullout-displacement curve confirms that interface shear mechanisms contribute to the pullout resistance

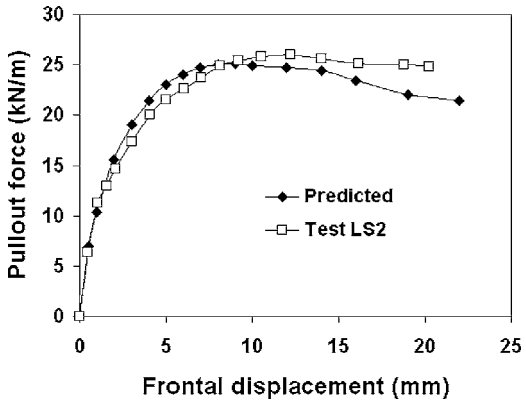

Fig. 19. Comparison between large-scale pullout test experimental results (Test LS2) and predictions

Table 4. Comparison between Experimental and Predicted Pullout Resistance from Large-Scale Tests

	Ultimate pullout resistance (kN/m)				
Test	LS1	LS2	LS3	LS4	LS5
Experimental value from large-scale pullout test	16.2	25.9	51.4	37.8	20.6
Value predicted using from individual-rib test results	14.8	24.7	52.0	38.1	22.6

for comparatively small displacements while passive mechanisms dominate the pullout resistance for comparatively large displacements. Although the basis for selection of the magnitude of the influence factor β requires further evaluation, it appears that the displacement at peak obtained from the transverse-rib pullout curves provide a good basis for such selection. As previously discussed, at least for the comparatively dense Geogrid G1 used in this study, the selection of the influence factor is not relevant when the objective of the prediction is to obtain the ultimate pullout resistance.

Table 4 summarizes the results obtained experimentally from large-scale pullout tests using Geogrid G1 and results predicted using the stress transfer model and individual-rib pullout test results. As for the case of the prediction of Test LS2 [Fig. 18(b)], the ultimate pullout resistance predicted for the other large-scale pullout tests with transverse ribs (Tests LS1, LS3, and LS4) were also obtained by neglecting the contribution of longitudinal ribs (i.e., considering $\beta=0$). The results summarized in Table 4 confirm that, for the conditions in this study, the ultimate pullout resistance is governed by the contribution of the transverse ribs and that data from individual-rib pullout tests can be used to predict the response of large-scale tests. Specifically, good predictions were obtained for pullout tests conducted using different geogrid lengths (350, 600, and 1,200 mm) as well as for pullout tests conducted under various normal stresses (25 and 50 kPa).

Conclusions

The contributions of longitudinal and transverse ribs to the overall pullout resistance of comparatively dense mesh geogrids were evaluated in this study. This investigation included the development of new devices to conduct longitudinal-rib and transverse-rib pullout tests on uneasily coated geogrids. In addition to the individual-rib pullout tests, the scope of the experimental program included large-scale pullout and tensile tests. A stress transfer model was implemented to predict the experimental results obtained from large-scale pullout tests using information collected from small-scale, individual-rib pullout tests. The main conclusions that can be drawn from this investigation are as follows:

- The newly developed small-scale, individual-rib pullout tests are expeditious and could be successfully used to provide a good estimate of the peak pullout resistance of the geogrids used in this study.
- Transverse geogrid ribs may cause significant oscillations of localized normal stresses during pullout testing. The stress redistribution appears to detrimentally affect the contribution of longitudinal ribs to the pullout resistance of geogrids, as verified for the dense mesh geogrids evaluated in this study.
- Experimental pullout test results and stress transfer analyses indicate that, at least for comparatively dense mesh geogrids, the interface shear mechanism contributes to the pullout force only for comparatively small displacements while the passive resistance mechanism governs the ultimate pullout resistance.
- Evaluation of the effect of transverse-rib spacing indicates that there is an optimum spacing below which interference between geogrid ribs leads to a decreased pullout resistance.
- The stress-transfer model implemented as part of this study allows prediction of the pullout resistance using input form individual-rib pullout tests and from tensile tests on geogrids. The use of an influence factors β greater than zero for comparatively small displacements is needed to obtain a good prediction of the entire pullout-displacement curve. However, at least for the comparatively dense mesh geogrid used in this study, the selection of the influence factor is not relevant for prediction of the ultimate pullout resistance.

Acknowledgments

The writers are thankful for the financial support received from FAPESP (State of Sao Paulo Sponsoring Agency) and the Department of Geotechnical Engineering of the University of Sao Paulo at Sao Carlos. Support received by the third writer from NSF under Grant No. CMS-0401494 is also gratefully acknowledged.

References

Alfaro, M. C., Miura, N., and Bergado, D. (1995). "Soil-geogrid reinforcement interaction by pullout and direct shear tests." *Geotech. Test. J.*, 18(2), 157–167.

ASTM. (2001a). "Standard test method for measuring geosynthetic pullout resistance in soil." *ASTM D 6706*, ASTM Book of Standards Volume, 04.13, Philadelphia.

ASTM. (2001b). "Test method for determining tensile properties of geogrids by the single or multi-rib tensile method." *ASTM D 6637*, ASTM Book of Standards Volume, 04.13, Philadelphia.

Bergado, D. T., and Chai, J. C. (1994). "Pullout force-displacement relationship of extensible grid reinforcement." *Geotext. Geomembr.*, 13(5), 295–316.

Bergado, D. T., Chai, J. C., Alfaro, M. C., and Balasubramaniam, A. S. (1994). *Improvement techniques of soft ground in subsiding and lowland environment*, A. A. Balkema, Rotterdam, The Netherlands.

Bergado, D. T., Shivashankar, R., Alfaro, M. C., Chai, J. C., and Balasubramaniam, A. S. (1993). "Interaction behavior of steel grid reinforcements in clayey sand." *Geotechnique*, 43(4), 589–603.

Chai, J. C. (1992). "Interaction between grid reinforcement and cohesive-frictional soil and performance of reinforced wall/embankment on soft ground." Ph.D. dissertation, Asian Institute of Technology, Bangkok, Thailand.

Dyer, M. R. (1985). "Observations of the stress distribution in crushed glass with applications to soil reinforcement." Ph.D. dissertation, Univ. of Oxford, Oxford, U.K.

Ingold, T. S. (1983). "Laboratory pull-out testing of grid reinforcements in sand." *Geotech. Test. J.*, 6, 101–111.

Jewell, R. A. (1990a). "Reinforcement bond capacity." *Geotechnique*, 40(3), 513–518.

Jewell, R. A. (1990b). "Strength and deformation in reinforced soil design." *Proc., 4th Int. Conf. on Geotextiles, Geomembranes and Re-*

lated Products, The Hague, The Netherlands, Vol. 3, 913–946.
Jewell, R. A. (1996). "Soil reinforcement with geotextiles." *Ciria Special Publication 123*, Thomas Telford Ltd., London.
Jewell, R. A., Milligan, G. W. E., Sarsby, R. W., and Dubois, D. (1984). "Interaction between soil and geogrids." *Proc., Symp. on Polymer Grid Reinforcement in Civil Engineering*, Science and Engineering Research Council and Netlon Limited, 18–30.
Koerner, R. M., Wayne, M. H., and Carroll, R. G., Jr. (1989). "Analytic behavior of geogrid anchorage." *Proc., Geosynthetics'89 Conf.*, IFAI, San Diego, 525–536.
Lopes, M. L., and Ladeira, M. (1996). "Influence of the confinement, soil density and displacement ratio on soil-geogrid interaction." *Geotext. Geomembr.*, 14(10), 543–554.
Milligan, G. W. E., Earl, R. F., and Bush, D. I. (1990). 'Observations of photo-elastic pullout tests on geotextiles and geogrids." *Proc., 4th Int. Conf. on Geotextiles, Geomembranes, and Related Products*, Vol. 2, The Hague, The Netherlands, 747–751.
Milligan, G. W. E., and Palmeira, E. M. (1987). "Prediction of bond between soil and reinforcement." *Symp. on Prediction and Performance in Geotechnical Engineering*, Calgary, Alta., Canada, 147–153.
Mitchell, J. K., Seed, R. B., and Seed, H. B. (1990). "Kettleman Hills waste landfill slope failure. I: Liner-system properties." *J. Geotech. Engrg.*, 116(4), 647–668.
Ochiai, H., Otani, J., Hayashic, S., and Hirai, T. (1996). "The pullout resistance of geogrids reinforced soil." *Geotext. Geomembr.*, 14(1), 19–42.
Palmeira, E. M. (1987). "The study of soil-reinforcement interaction by means of large scale laboratory tests." Ph.D. dissertation, Univ. of Oxford, Oxford, U.K.
Palmeira, E. M. (2004). "Bearing force mobilisation in pull-out tests on geogrids." *Geotext. Geomembr.*, 22(6), 481–509.
Palmeira, E. M., and Milligan, G. W. E. (1989a). "Large-scale direct shear tests on reinforced soil." *Soils Found.*, 29(1), 18–30.
Palmeira, E. M., and Milligan, G. W. E. (1989b). "Scale and other factors affecting the results of the pullout tests of grids buried in sand." *Geotechnique*, 39(3), 551–584.
Peterson, L. M., and Anderson, L. R. (1980). "Pullout resistance of welded wire mats embedded in soil." *Research Rep., Submitted to Hilfiker Co.*, Civil and Environmental Engineering Dept., Utah State Univ., Logan, Utah.
Raju, D. M., Lo, S. C. R., Gopalan, M., and Gao, J. (1998). "On large-scale laboratory pull-out testing." *Geotech. Eng.*, 29(2), 123–155.
Sarsby, R. W. (1985). "The influence of aperture size/particle size on efficiency of grid reinforcement." *Proc., 2nd Canadian Symp. on Geotextiles and Geomembranes*, Edmonton, Alta., Canada, 7–12.
Sugimoto, M., Alagiyawanna, A. M. N., and Kadoguchi, K. (2001). "Influence of rigid and flexible face on geogrid pullout tests." *Geotext. Geomembr.*, 19(5), 257–328.
Teixeira, S. H. C. (1999). "Construction and calibration of a large pullout test device, MS dissertation, Dept. of Geotechnical Engineering, Univ. of Sao Paulo at Sao Carlos (in Portuguese).
Teixeira, S. H. C., and Bueno, B. S. (1999). "An equipment for pullout test of geosynthetics." *Geossintéticos' 99*, Rio de Janeiro, 215–222 (in Portuguese).
Wilson-Fahmy, R., and Koerner, R. M. (1993). "Finite element modeling of soil-geogrid interaction in pullout loading conditions." *Geotext. Geomembr.*, 12(5), 479–501.